2-D Modes Analysis of Micro-Ring Resonator: In case of chemical vapor sensing

Harry Ramza[1], Emas Fiqry Nurdwiprasetio[1], Aditya Ervansyah[1]
Sugianto[2], Saeed Salem Bahashwan[3], Mohd Haris Md Khir[3]

1. Department of Electrical Engineering, Faculty of Engineering, Universitas Muhammadiyah Prof. Dr. Hamka
Jalan Tanah Merdeka No. 6, Jakarta 14560 INDONESIA
E-mail: hramza@uhamka.ac.id; emasfyqri11@gmail.com; aden23adit@gmail.com
2. Department of Physics Education, Faculty of Pedagogy and Teacher Training
Universitas Muhammadiyah Prof. Dr. Hamka
Jalan Tanah Merdeka No. 12, Jakarta 14560 INDONESIA
E-mail: s.arjo@uhamka.ac.id
3. Department of Electric and Electronic, Universiti Teknologi PETRONAS
Bandar Seri Iskandar, Tronoh, Perak,31750 MALAYSIA
E-mail: saeedsb2013@gmail.com; harisk@utp.edu.my

2020 8th International Conference on Intelligent and Advanced Systems (ICIAS) | 978-1-7281-7666-6/21/$31.00 ©2021 IEEE | DOI: 10.1109/ICIAS49414.2021.9642688

***Abstract*-This paper describes 2-D modes analysis on the waveguide structure. Micro - Ring Resonator formation was simulated to able the chemical vapor detection by using COMSOL Multiphysics application. We present the simulation of mode analysis from a Micro-ring Resonator as sensing the chemical vapor. By implementing the device parameters. We have seen from the simulator that the optical mode is handled equally within the ring. Using the variation of effective refractive index, our simulator result of ring resonator generated the mode analysis in two-dimension perspective. We conclude that the ring resonator device has potential for generating the certain wavelength.**

Keywords: 2-D Mode analysis, Micro - Ring Resonator, COMSOL Multiphysics

I. INTRODUCTION

Optical waveguide well known as a dielectric waveguide are structures that applied to confine and guided the light. Some of common materials are used and their refractive index is listed on the figure 1. The guidance function depends on the difference of refractive index between the waveguiding area (core) and the surrounding area of other media (cover).

The light is confined from the high refractive index region and the waveguiding region along the material structures caused the total internal reflection. The principle materials used to produce the optical waveguide are fused silica (SiO_2) that is a high-silica glass for optical fiber, lithium niobate ($LiNbO_3$) that is a ferroelectric insulating crystal, gallium arsenide (GaAs) and Indium phosphate (InP) that is a semiconductor material for integrated optical circuits[1].

Modeling and analysis of waveguide devices are essential to design and prediction of the possible performance from fabrication parameters. The "modeling" usually refers to a process in which a device made of particular material and by specific fabrication technique is modeled based on physical principles and approximations.

TABLE I
REFRACTIVE INDEX (n) OF OPTICAL WAVEGUIDE MATERIALS

Dielectric Material	λ (μm)	*n* (Refractive Index)
Fused Silica (SiO_2)	0.633	1.46
Typical Microscope Slide glass	0.633	1.51
Sputtered Corning 7059 glass	0.633	1.62
$LiTaO_3$ (n_0)	0.80	2.15
$LiTaO_3$ (n_{eff})	0.80	2.16
$LiNbO_3$ (n_0)	0.80	2.28
$LiNbO_3$ (n_c)	0.80	2.19
GaAs	0.90	3.6
InP	1.51	3.17

In the context of guided wave optoelectronics and fiber optics, a geometric configuration and / or a refractive index are determinate. The mathematical model is then analyzed analytically or numerically and the understanding and prediction of the material properties of the actual device depend on the analysis of the model.

The physical intuition is often required for the alternative of the right model which is sufficient for the application and appropriate for the analysis. In principle, the problem is defined by a domain D or electric flux density domain in which Maxwell equation need to be solved taking into account the continuity and boundary conditions. Furthermore, a micro-ring complex device may be modeled and analyzed structurally and / or functionally as a system of some simple constituent element. There are many techniques to produce the refractive index profile required by the optical waveguide. The optional special techniques depend on the material used to be applied, the application requested and the facilities available.

This paper describes the optical waveguide mode analysis from a micro-ring resonator that deposited the silica glass material into the silicon oxide through the deposition. In this part, the optical mode from the silica glass also looks at causing the interaction of ammonia vapor (NH_3). Analysis performed by simulation methods generated and the analysis performed by simulation methods generated from the application of the COMSOL Simulator.

II. THEORY

Mode (or normal mode) of an optical waveguide is set of Eigen solutions to the boundary value problem governed by the Maxwell equations of frequency domain and the boundary conditions for a specific waveguiding structure. For a uniform waveguide, the refractive index $n = n(x, y)$ does not depend on z (the waveguide is translationally invariant). Then the electric and magnetic fields of the waveguide may be expressed as a linear superposition of fields with separable form,

$$E_i(r) = \hat{E}_i(x, y)\, e^{-j\beta_i z} \quad (1)$$

$$H_i(r) = \hat{H}_i(x, y)\, e^{-j\beta_i z} \quad (2)$$

where β_i is the propagation constant of the i-th mode. The phase velocity of each mode is given in terms of the propagation constant as

$$v_{pi} = \frac{\omega}{\beta_i} \quad (3)$$

and the group velocity,

$$v_{gi} = \frac{\partial \omega}{\partial \beta_i} \quad (4)$$

Furthermore, we can decompose the field into transversal and longitudinal components, such as

$$\hat{E} = \hat{E}_t + \hat{E}_z \quad (5)$$

$$\hat{H} = \hat{H}_t + \hat{H}_z \quad (6)$$

where the subscript t stands for the transversal (x or y) component. Substitute equation (1) and (2) into the Maxwell equation,

$$\nabla \times E = -j\omega\mu H \quad (7)$$

$$\nabla \cdot (\epsilon E) = 0 \quad (8)$$

The following equations are derived,

$$\nabla_t \times \hat{E}_z - j\beta\hat{z} \times \hat{E}_t = -j\omega\mu_0\hat{H}_t \quad (9.a)$$

$$\nabla_t \times \hat{H}_z - j\beta\hat{z} \times \hat{H}_t = j\omega n^2\epsilon_0\hat{E}_t \quad (9.b)$$

and

$$\nabla_t \times \hat{E}_t = -j\omega\mu_0\hat{H}_z \quad (10.a)$$

$$\nabla_t \times \hat{H}_t = j\omega n^2\epsilon_0\hat{E}_z \quad (10.b)$$

Mode of 2-D Structure.

A direct observation of eq (9) and (10) reveals the following symmetry properties of the mode on uniform waveguide. For two-dimensional waveguide structures, the electromagnetic fields do not vary with y, in example,

$$\frac{\partial}{\partial y} = 0 \quad (11)$$

By substitute this condition into eq (10), we derive;

TE Mode[2]

$$\frac{\partial^2 \hat{E}_y}{\partial x^2} + \left(n^2 {k_0}^2 - \beta^2\right)\hat{E}_y = 0 \quad (12)$$

$$\hat{H}_x = -\frac{\beta}{\omega\mu_0}\hat{E}_y \quad (13)$$

$$\hat{H}_z = \frac{j}{\omega\mu_0}\frac{d\hat{E}_y}{dx} \quad (14)$$

TM Mode

$$\frac{\partial^2 \hat{H}_y}{\partial x^2} + \left(n^2 {k_0}^2 - \beta^2\right)\hat{H}_y = 0 \quad (15)$$

$$\hat{E}_x = \frac{\beta}{n^2\omega\epsilon_0}\hat{H}_y \quad (16)$$

$$\hat{E}_z = -\frac{j}{n^2\omega\epsilon_0}\frac{d\hat{H}_y}{dx} \quad (17)$$

where $n = n(x)$. Therefore, the TE and TM modes are completely decoupled for the 2D structures. Also, for the case of plane wave solutions in interface of reflections and transmission, the two sets equations are dual to each other. One may obtain the solutions for the TE mode from the TM mode by replacing $\hat{E}$ for $\hat{H}$, $\hat{H}$ for $-\hat{E}$ and ϵ for μ and vice versa.

Micro-ring Resonator

The ring resonators play an important role in the success of photonic silicon technology because of silicon material enables the resonance of wavelength with an unprecedented small dimension [3]. A ring resonator consists of an optical waveguide that is looped back on itself, such that the resonance occurs when the optical path length is exactly all the number of wavelengths as seen in figure 1. Therefore, the ring resonator are support all the multiple resonance and the spacing between these resonances, free spectral range (FSR) depends on the resonator length.

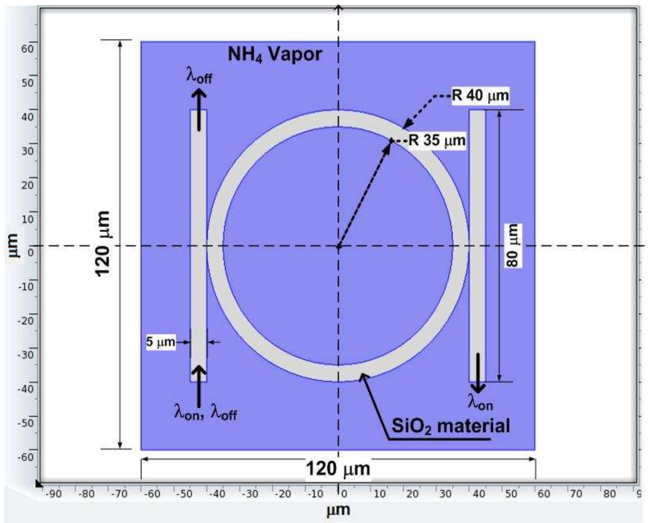

Figure 1. Optical Ring Resonator

Fundamental of ring resonator can be studied by determining a dielectric ring that embedded on the dielectric material with smallest refractive index as shown if figure 1. The optical field is joined into the ring that it is conditions and reflection of the light will transmit perennially on the ring limit with smallest refractive index that nearby to the material.

III. Initial Parameters

Parameters of micro-ring resonator is FSR, it is explained as a part of frequency of two sequences resonance. This is can be closed in by following amount of m and non-dispersive material expressed as[4, 5],

$$\lambda_m = \frac{2\pi R n_{eff}}{m} \tag{18}$$

$$\Delta f = \frac{c}{2\pi\ R\ n_{eff}} \tag{19}$$

In the wavelength, it can be

$$\Delta\lambda = \frac{\lambda^2}{2\pi\ R\ n_{eff}} \tag{20}$$

where λ is wavelength at the vacuum. The single ring of optical resonator with two waveguide signal (see figure 1) in left side of signal named input bus and the right side is named as output bus. Bandwidth of resonance is one of critical parameter for micro-ring and it offers the equation,

$$F = \frac{FSR}{\Delta\lambda_{\mathrm{FWHM}}} \tag{21}$$

$\Delta\lambda$ is explained as the bandwidth of resonance (full width half maximum) and it was evinced to be,

$$\Delta\lambda = \frac{2\kappa^2\lambda^2 v_g}{(2\pi)^2 RC} = \frac{2\kappa^2\lambda^2}{(2\pi)^2 R\ n_{eff}} \tag{22}$$

where κ is coupling efficiency that will discussed by using the couple mode theory and equation (22) generates group of velocity (v_g) approach to phase velocity (c/n_{eff}), we neglect the effect of dispersive for simplifications.

Quality or Q – factor for a ring resonator is a sensitivity of frequency structure[6]. The result of this difference has the largest effect on quality factor of the ring resonator that is defined in equation (23) below, where L_{eff} as the effective length and λ as the wavelength center of resonator [7].

$$Q = \frac{\pi\ L_{eff}\ n_{eff}}{\lambda\ \cos^{-1}\left(\frac{1 + t^4\ \alpha^2 - 4t^2\alpha}{-2t^2\ \alpha}\right)} \tag{23}$$

It is often useful for individual channel on the micro-ring waveguide to have a similar response in devices such couplers and filters.

IV. Mode Analysis

This paper explains the TE (transverse electric) mode analysis on the micro – ring resonator device. It has the initial condition as like as[2, 8],

$$E_z = 0\ \ and\ \ H_z \neq 0 \tag{24}$$

then the existing components based on equation (24) are E_X, E_Y and H_z. The results of mode only present the value of components E_X and H_z in each point of coordinate from micro – ring resonator device. As seen in figure 2, it shows the difference of mode numbers that create the difference of electric field in the x-direction and magnetic field in the z-direction.

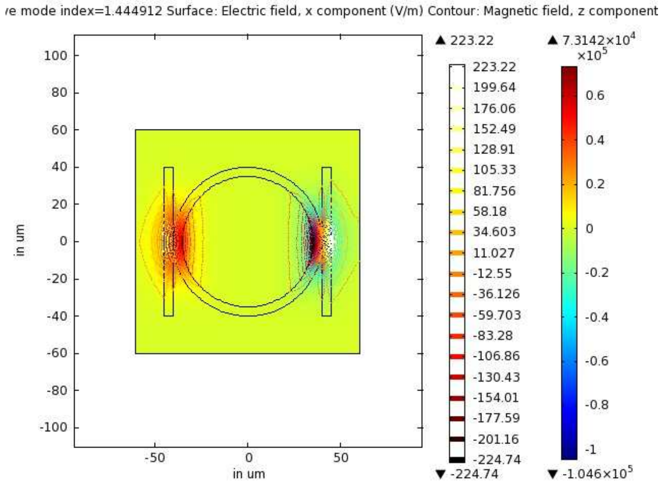

(a)

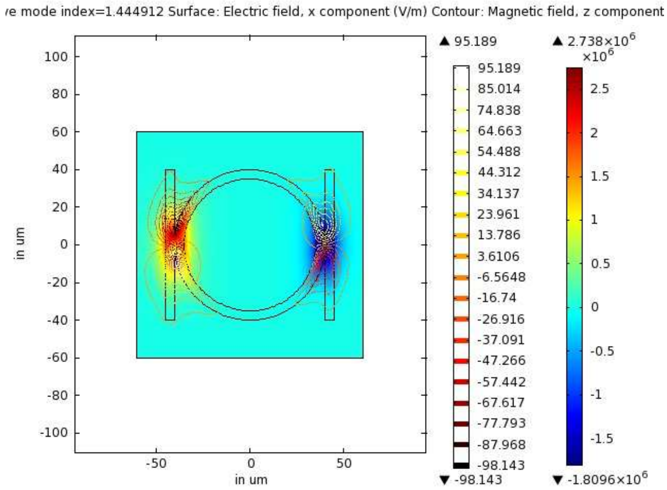

(b)

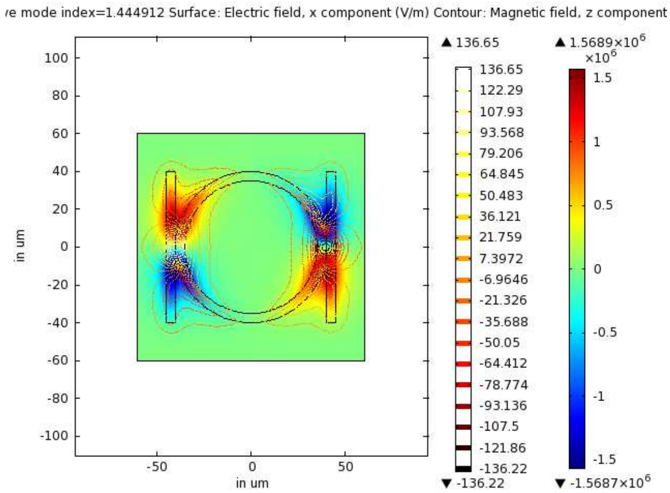

(c)

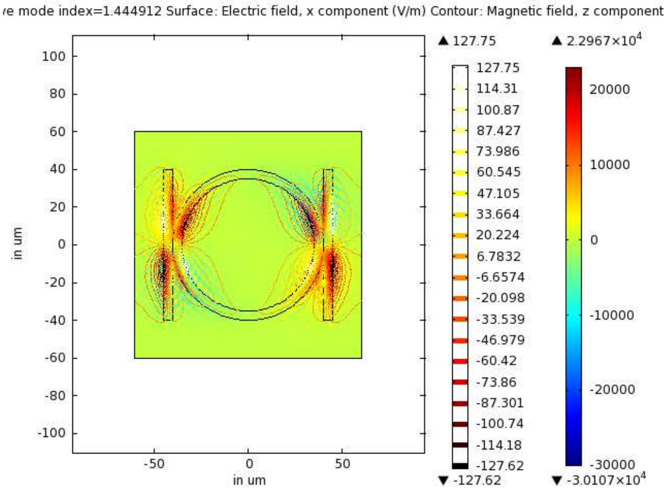

(d)

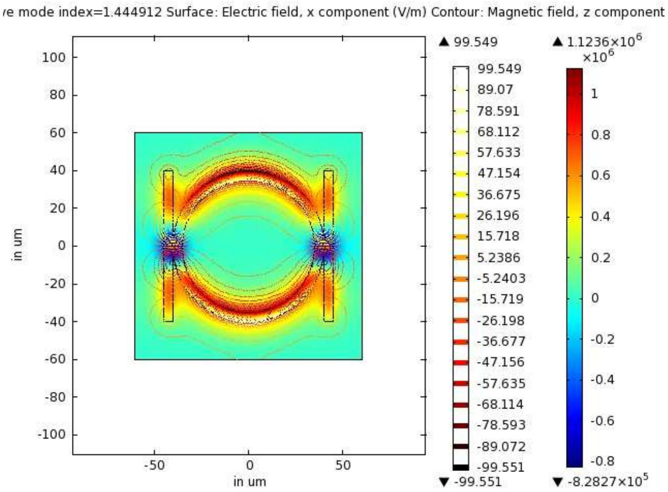

(e)

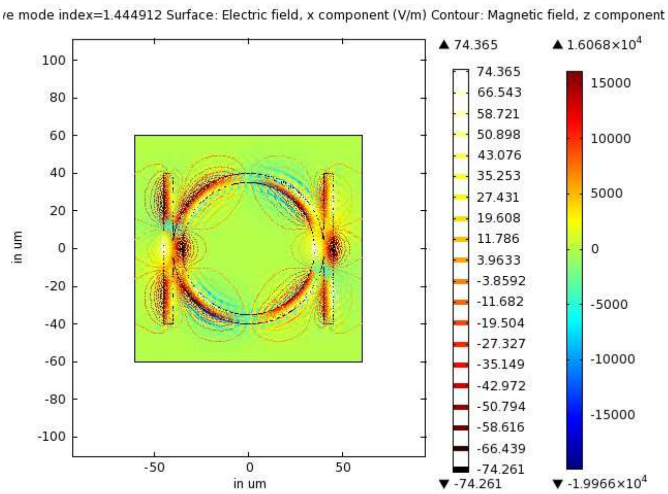

(f)

Figure 2. TE Mode pattern with; (a). Number of mode = 1; (b). Number of mode = 2; (c). Number of mode = 5; (d). Number of mode = 8; (e). Number of mode = 9; (f). Number of mode = 10.

From figure 2 (a), (b), and (c) shows the mode pattern with the smaller number of modes tends to create the propagation around the junction between the two-hand and the ring position. It is the phenomenon of the light-wave propagation from the left hand or the right hand to the ring device as a resonator. In case of greater the number of modes; the light wave propagation will shift from the hand part into the ring part. This situation as seen as figure 2 (d), (e) and (f).

The figure 3, 4, 5 and 6 shows the electric field and the magnetic field movement on the left hand of micro – ring based on the figure 1. Propagation wave position on the left side or upper left hand is amount 42.50 µm from the center point.

Simulation result is seen the proportional of TE (Transverse Electric) propagating mode. The propagation describes the electric field in x – component (Ex) and the magnetic field in z – component (Hz).

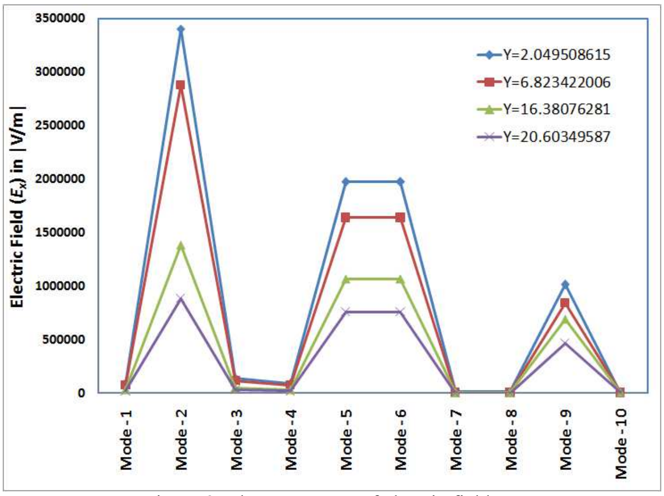

Figure 3. The movement of electric field x-component (Ex) in each number of modes

As seen in figure 3, the electric field propagation value of the x – component with the increment in the number of modes shows a quite significant difference from mode – 2, 5, 6 and 9. The value of the electric field | Ex | is an absolute value in Volt/meter. The results of this simulation distinguish four propagation points at the y – coordinate (upper left side in figure 1), namely 2.049508615 µm, 6.823422006 µm, 16.38076281 µm, and 20.60349587 µm.

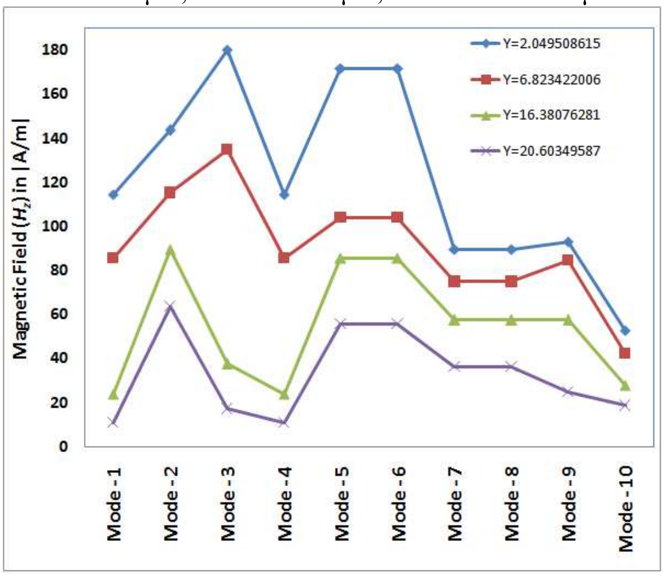

Figure 4. The movement of magnetic field z-component (H_z) in each number of modes

In likewise, figure 4 describes the magnetic field for z – component (Hz) with the highest movement value at y – coordinate around 2.049508615 μm. The propagation format will perform the same pattern on the lower left hand, upper right hand and lower right hand from the micro – ring resonator in figure 1.

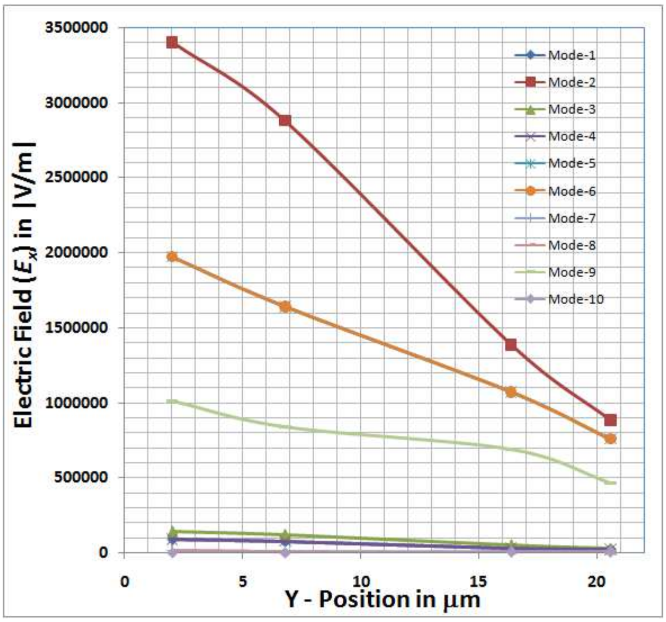

Figure 6. The movement of electric field x-component (E_x) in Y-position of Micro-ring

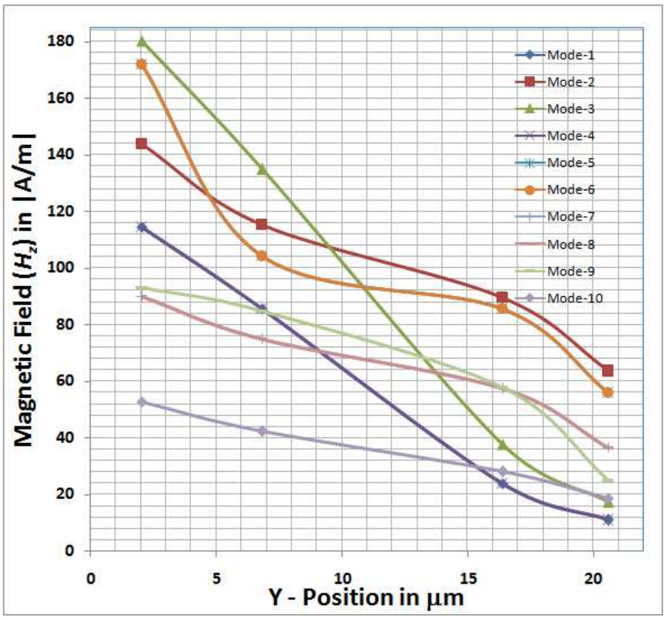

Figure 7. The movement of magnetic field z-component (H_z) in Y-position of Micro-ring

Figure 6 above explains the condition of the electric field (Ex) on each four-position point's movement from y – coordinate from the upper left hand (base on the figure 1) micro – ring resonator. This result is an absolute value on each variant of the number of modes that it was produced.

Likewise with Figure 7 above the motion of magnetic field on the z – component corresponds to the movement position of y – axis (upper left arm of the micro ring resonator).

V. CONCLUSION

The mode propagation is determined by the position point of x – the coordinate amount of -42.5 μm. It means that the arm of micro – ring resonator existed on the left side. The number of modes was simulated around 10 modes with the variant value of different points from y – coordinates are 2.049508615 μm, 6.82342 μm, 16.38076281 μm and 20.603495 μm.

ACKNOWLEDGMENT

This project has been carried out in Optical Engineering and Device research group laboratory under the Department of Electrical Engineering., Universitas Muhammadiyah Prof. Dr. HAMKA, Jakarta, Indonesia (UHAMKA). This project is part of a collaborative research between Universiti Petronas Perak, Malaysia (UTP) and Universitas Muhammadiyah Prof. Dr. HAMKA (UHAMKA).

REFERENCES

[1]. A. Yariv and P. Yeh, *Optical Waves in Crystals: Propagation and Control of Laser Radiation*: Wiley, 2002, ISBN: 9780471430810.

[2]. D. Marcuse, *Theory of Dielectric Optical Waveguides*: Elsevier Science, 2013, ISBN: 9780323162364.

[3]. W. Bogaerts, P. De Heyn, T. Van Vaerenbergh, K. De Vos, S. Kumar Selvaraja, T. Claes, P. Dumon, P. Bienstman, D. Van Thourhout, and R. Baets, 2012, "Silicon microring resonators," *Laser & Photonics Reviews,* Vol. 6, No. 1, pp. 47-73. DOI: 10.1002/lpor.201100017.

[4]. B. Mulyanti, H. Ramza, R. E. Pawinanto, J. A. Rahman, M. S. Ab-Rahman, W. S. Putro, L. Hasanah, and A. B. Pantjawati, 2017, "Micro – ring resonator with variety of gap width for acid rain sensing application: preliminary study," *Journal of Physics: Conference Series,* Vol. 852, pp. 012043. DOI: 10.1088/1742-6596/852/1/012043.

[5]. B. E. Little, S. T. Chu, H. A. Haus, J. Foresi, and J. Laine, 1997, "Microring resonator channel dropping filters," *Journal of Lightwave Technology,* Vol. 15, No. 6, pp. 998-1005. DOI: 10.1109/50.588673.

[6]. H. Han, B. Xiang, and J. Zhang, 2018, "Simulation and Analysis of Single-Mode Microring Resonators in Lithium Niobate Thin Films," *Crystals,* Vol. 8, No. 9, pp. 342.

[7]. A. Vorckel, M. Monster, W. Henschel, P. H. Bolivar, and H. Kurz, 2003, "Asymmetrically Coupled Silicon-On-Insulator Microring resonators for compact add - drop Multiplexers," *IEEE Photon. Technol. Lett,* Vol. 15, No. 7, pp. 921-923.

[8]. M. K. Chin and S. T. Ho, 1998, "Design and modeling of waveguide-coupled single-mode microring resonators," *Journal of Lightwave Technology,* Vol. 16, No. 8, pp. 1433-1446. DOI: 10.1109/50.704609.